Mori *et al. Earth, Planets and Space* (2016) 68:49
DOI 10.1186/s40623-016-0418-0

Earth, Planets and Space

FULL PAPER

Open Access

Volcanic plume measurements using a UAV for the 2014 Mt. Ontake eruption

Toshiya Mori[1*], Takeshi Hashimoto[2], Akihiko Terada[3], Mitsuhiro Yoshimoto[4], Ryunosuke Kazahaya[5], Hiroshi Shinohara[5] and Ryo Tanaka[6]

Abstract

A phreatic eruption of Mt. Ontake, Japan, started abruptly on September 27, 2014, and caused the worst volcanic calamity in recent 70 years in Japan. We conducted volcanic plume surveys using an electric multirotor unmanned aerial vehicle to elucidate the conditions of Mt. Ontake's plume, which is flowing over 3000 m altitude. A plume gas composition, sulfur dioxide flux and thermal image measurements and a particle sampling were carried out using the unmanned aerial vehicle for three field campaigns on November 20 and 21, 2014, and June 2, 2015. Together with the results of manned helicopter and aircraft observations, we revealed that the plume of Mt. Ontake was not directly emitted from the magma but was influenced by hydrothermal system, and observed SO_2/H_2S molar ratios were decreasing after the eruption. High SO_2 flux of >2000 t/d observed at least until 20 h after the onset of the eruption implies significant input of magmatic gas and the flux quickly decreased to about 130 t/d in 2 months. In contrast, H_2S fluxes retrieved using SO_2/H_2S ratio and SO_2 flux showed significantly high level of 700–800 t/d, which continued at least between 2 weeks and 2 months after the eruption. This is a peculiar feature of the 2014 Mt. Ontake eruption. Considering the trends of the flux changes of SO_2 and H_2S, we presume that majority of SO_2 and H_2S are supplied, respectively, from high-temperature magmatic fluid of a deep origin and from hydrothermal system. From the point of view of SO_2/H_2S ratios and fumarolic temperatures, the plume degassing trend after the 2014 eruption is following the similar course as that after the 1979 eruptions, and we speculate the 2014 eruptive activity will cease slowly similar to the 1979 eruption.

Keywords: Mt. Ontake, The 2014 eruption, Phreatic eruption, Volcanic plume, Sulfur dioxide, Hydrogen sulfide, Volcanic gas flux, UAV, MultiGAS

Background

Volcanoes often change their eruption styles during a course of eruptive activity. Transition from phreatic eruptions to climactic magmatic eruptions is one of the style changes observed. Although only about 13 % of phreatic eruptions had been reported to transition from phreatic to magmatic or phreatomagmatic eruptions (Barberi et al. 1992), Barberi et al. (1992) also speculate that the above number is a minimum value because relatively minor phreatic activities preceding the major magmatic eruption could have been potentially overlooked by the original reporters. In monitoring of volcanoes, detection of a precursory process for a volcanic eruption is an important aspect. Similarly, elucidation of the conditions of the activities for an erupted volcano and of the prospect of the ongoing eruptive activity is also important matters. Thus, the monitoring of an eruptive activity that started in a phreatic manner needs careful attention whether the activity diminishes or becomes more vigorous toward magmatic activities.

Volcanic gas composition and flux are generally influenced by changes in magma degassing and/or the hydrothermal system beneath the volcano. They can provide crucial information in understanding such subsurface processes, and therefore, they are considered useful tools for volcano monitoring. According to volcanic gas surveys of pioneering researchers, volcanic and/or fumarolic

*Correspondence: mori@eqchem.s.u-tokyo.ac.jp
[1] Geochemical Research Center, Graduate School of Science, The University of Tokyo, 7-3-1 Hongo, Bunkyo-ku, Tokyo 113-0033, Japan
Full list of author information is available at the end of the article

gas composition varies with outlet temperature, and there is a general trend that SO_2 is a dominant S-bearing gas for high outlet temperature, whereas H_2S becomes dominant for low outlet temperature (e.g., Iwasaki et al. 1966). For example, major degassing Japanese volcanoes that emit high-temperature magmatic gases usually have SO_2/H_2S molar ratio >6 (Shinohara 2013). On the one hand, volcanic gases influenced by hydrothermal system generally have lower temperatures and lower to negligible SO_2/H_2S molar ratios (e.g., Iwasaki et al. 1966).

From a thermodynamical point of view, SO_2 and H_2S abundances are controlled by the following chemical equation

$$H_2S + 2H_2O = SO_2 + 3H_2 \quad (1)$$

and SO_2/H_2S ratio depends on temperature, pressure and redox conditions (Giggenbach 1987), in which high temperature favors high SO_2/H_2S ratio at low-pressure conditions. Thus, it is generally considered that SO_2 and H_2S are indicators of magmatic and hydrothermal contributions, respectively (Oppenheimer 2003) and that increase in the SO_2/H_2S ratio corresponds to increasing magmatic influence, and vice versa. However, in reality, it is difficult to judge the influence of magmatic or hydrothermal fluids just from increase or decrease in the SO_2/H_2S molar ratio. The ratio can increase without input of magmatic fluid (Aiuppa et al. 2006) or can decrease without considering an elevated influence of hydrothermal system (Shinohara 2013). The chemistry of sulfur for volcanic gas, especially related to hydrothermal system, is very complicated (Symonds et al. 2001). As SO_2 is considered to be a possible magmatic indicator, continuing high SO_2 emission rate (>100 t/d) alone can be a good indicator of magmatic intrusion (Symonds et al. 2001). Sulfur dioxide (SO_2) can be easily scrubbed from uprising volcanic gas by interaction with hydrothermal and groundwater systems, whereas extraction of SO_2 from SO_2-absorbed hydrothermal fluids is difficult (Symonds et al. 2001). Thus, high emission of SO_2 is basically unlikely without input of SO_2 from the depth.

A measurement of SO_2 emission for volcanic plume is quite easily accomplished by using a miniature UV spectrometers (Galle et al. 2003; Horton et al. 2006; Mori et al. 2007). These instruments can be used remotely from a safe distance and can be used even during an eruptive period. In contrast, there is no practical way to measure H_2S from a remote distance from the plume. Although remote FTIR observation for volcanic gas (e.g., Mori and Notsu 1997; Burton et al. 2000) can measure many volcanic gas species including SO_2 from a safe distance, there has been no report of H_2S detection (Oppenheimer et al. 2011). Thus, at least for measuring SO_2/H_2S ratio, there is no other practical way except for in-plume direct measurements. MultiGAS (Shinohara 2005; Aiuppa et al. 2005a, b) or VERP (Kelly et al. 2013) that are equipped by electrochemical SO_2 and H_2S sensors is suitable systems to measure SO_2/H_2S ratio inside the plume. For example, VERP onboard manned aircraft was used for measuring volcanic gas chemistry including SO_2/H_2S ratios inside the eruptive plume of Redoubt volcano (Werner et al. 2013). However, measurements using a manned aircraft into volcanic plumes are quite limited considering safety concerns and should be replaced if supplemental methods are available.

The recent progress of UAV technology is remarkable, and the UAVs are now advancing into volcanological and geological fieldworks (e.g., McGonigle et al. 2008; Kaneko et al. 2011; Shinohara 2013; Amici et al. 2013; Jordan 2015). The advantage of using UAVs in volcanology, especially in volcanic plume monitoring, is significant to avoid the risks of researchers and to obtain data from unapproachable locations such as inside a dense plume or an active crater. The first pioneering work using a remote-controlled engine helicopter for volcanic plume measurement was carried out at La Fossa Crater, Vulcano, Italy, measuring SO_2 flux with a miniature UV spectrometer and CO_2/SO_2 ratio with a simplified MultiGAS (McGonigle et al. 2008). Shinohara (2013) made MultiGAS measurements with a fixed-wing UAV for the volcanic plume of Shinmoedake volcano, Japan, during a repeating Vulcanian eruption stage. For volcanoes with hydrothermal influence, monitoring of both SO_2 and H_2S in volcanic plumes is important. Unlike SO_2, remote monitoring of H_2S is currently impossible, and thus, measurement of H_2S for highly active volcanoes is generally difficult. The use of UAVs is expected to overcome such difficulties more simply and safely.

In this paper, we present the results of volcanic plume survey using an electric multirotor UAV for the volcanic plume of Mt. Ontake volcano, Japan, to elucidate the conditions of volcanic activity after the phreatic explosion on September 27, 2014. For this purpose, we carried out SO_2 flux measurements, MultiGAS measurements, thermal imaging for plume vents and particle sampling inside the plume on November 20 and 21, 2014, and on June 2, 2015, using a multirotor UAV. Together with the results of a manned helicopter and aircraft measurements, we estimate the gas emission conditions of Mt. Ontake and also compare the observed results with those for the 1979 eruption of the volcano.

Mt. Ontake volcano

Mt. Ontake volcano (3067 m a.s.l.) is a stratovolcano in the central part of Honshu Island, Japan (Fig. 1). According to historical materials, there had been continuous weak fumarolic activity at Jigokudani area (Fig. 1) at least

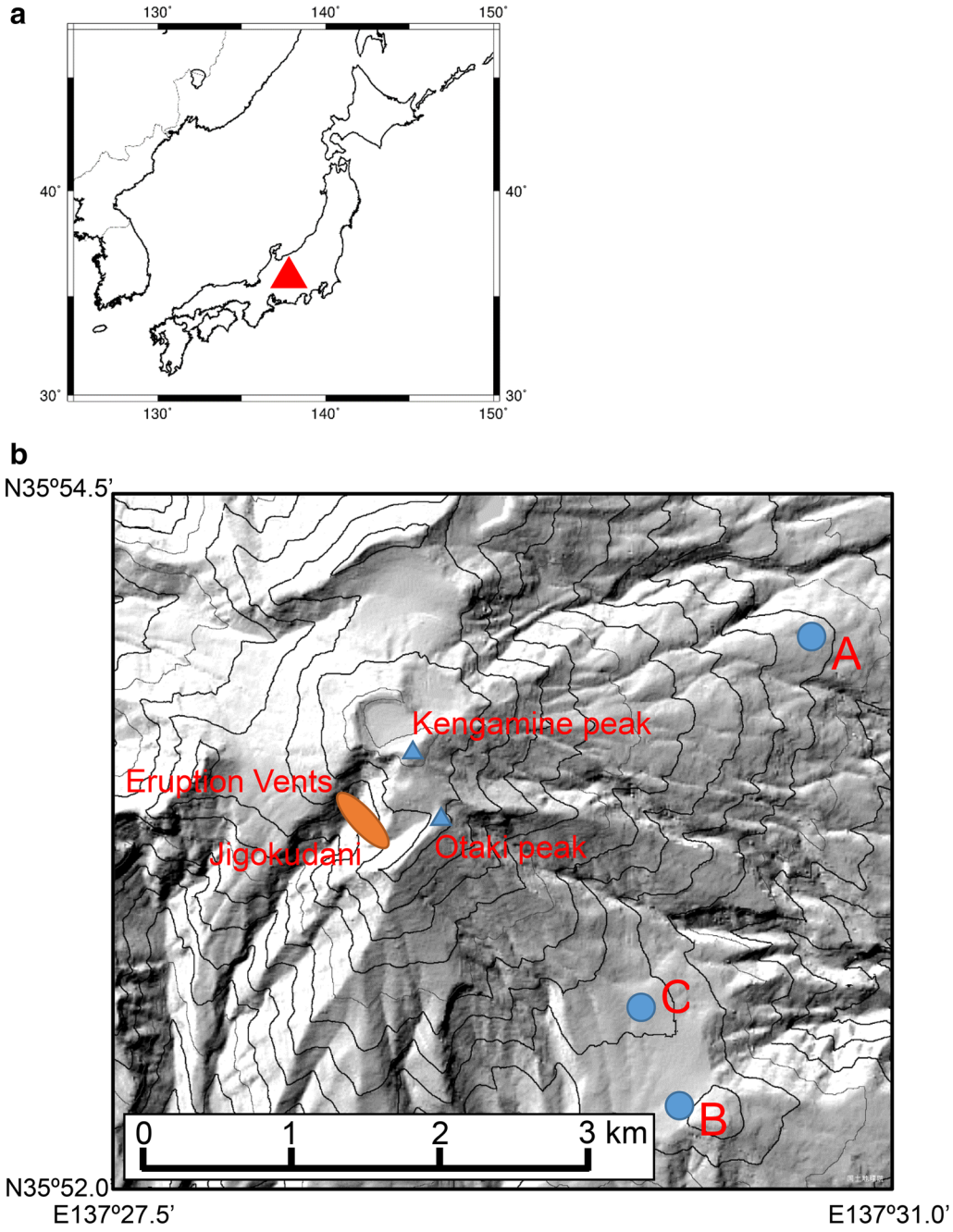

Fig. 1 **a** A map of Japan showing the location of Mt. Ontake (*solid triangle*) in the central part of Japan. **b** A map of Mt. Ontake showing the locations of the summit peaks, eruption vents area (*orange area*). Kengamine (*solid triangle*) is the highest peak of Mt. Ontake (3067 m), and Otaki (*triangle*) is a peak about 500 m southeast of Kengamine. The 2014 eruption of Mt. Ontake volcano occurred from multiple vents (Eruption vents area) in Jigokudani area, southwest of Kengamine peak. *Solid circles A*, *B* and *C* are taking off and landing points, respectively, for the campaigns on November 20 and 21, 2014, and June 2, 2015. Contours are drawn every 100 m. The map was drawn with Kashmir 3D software (http://www.kashmir3d.com) using 10 m mesh DEM data of Geospatial Information Authority of Japan

for last 250 years (Oikawa 2008). However, as a historical eruption, this volcano had been dormant until the 1979 eruption (Oikawa 2013). Recent studies revealed several magmatic eruptions and more frequent phreatic eruptions in last 10,000 years (Suzuki et al. 2007, 2009; Oikawa and Okuno 2009). The 1979 eruption of

Mt. Ontake started at around 5:20 (JST) on October 28, 1979, from NW–SE aligned new vents at Jigokudani on the upper southern flank (~2700 m a.s.l.) of the volcano (Kobayashi 1979; Soya et al. 1980; Ossaka et al. 1983). The eruption emitted 0.95–1.23 $\times$ 10^9 kg of ash (Maeno et al. 2014), which was detected up to 130 km of distance (Ossaka et al. 1983). Between 1979 and 2014, there were two small-scale eruptions in 1991 and 2007 using the vents of the 1979 eruption (Oikawa 2013). In 1984, a debris avalanche occurred on the SSE flank of the volcano due to the 1984 Western Nagano Earthquake (M6.8) and the avalanche went down about 10 km causing a great disaster to the local area (Oikawa 2013).

The 2014 eruption of Mt. Ontake occurred at around 11:52 (JST) on September 27, 2014, from Jigokudani area. Although precursory increase in the seismicity was detected about 2 weeks before the eruption, there was no significant volcanic tremor or deformation until about 10 min before the onset of the eruption (Kato et al. 2015). The eruption was a phreatic one, and the eruption column went up about 9 km and a low-temperature pyroclastic flow went down 2.5 km on the SW flank of the volcano (JMA 2014a). Total amount of pyroclastic material during the eruptions ranged 0.41–1.03 $\times$ 10^9 kg and was similar to the 1979 eruption (Maeno et al. 2014). At the time of the eruption, many hikers were close to the summit area because of the optimal weather condition on the day and the coincidence with lunch time (Yamaoka 2015). This caused the worst volcanic calamity in the last 70 years in Japan, in which 58 people were killed and five people went missing.

Ash emission continued until 10 October (JMA 2014b) after the eruption on 27 September. Number of volcanic earthquakes and SO_2 flux quickly decreased in the first 2 weeks (JMA 2014b), and a continuous contracting deformation has been observed by GNSS after October 2014 (JMA 2015). As of October 2015, the activity of Mt. Ontake has been gradually wanning after the single eruption on September 27, 2014, and it did not transition to magmatic or phreatomagmatic activities.

Methods

The UAV used in the observation was an eight-rotor multirotor drone αUAV series (Amuse Oneself Inc., Japan, Fig. 2a) operated by the company. The UAV is controlled by a pilot during takeoff and landing and is automatically navigated with GNSS between prefixed waypoints. In the observation at Mt. Ontake, our requirements for the UAV flights were as follows: (1) roundtrip flight of 8 km; (2) flight at altitude over 3000 m; (3) flight with a relative elevation of more than 1000 m; and (4) flight into a dense volcanic plume. For the flight requirements above, we were requested to have maximum payload of about 1 kg

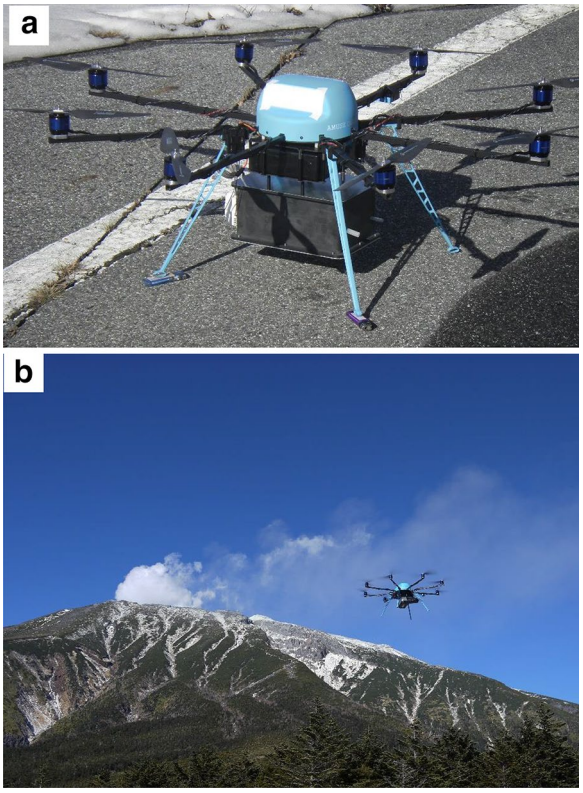

Fig. 2 **a** Photograph of the multirotor UAV (αUAV series) used in the campaigns with the MultiGAS box (*black box*) attached under it. A white adhesive sheet-type dust sampler was attached on the green body of the UAV. The photograph was taken on November 20, 2014, before the flight. **b** Photograph of the UAV just after taking off from point B (Fig. 1b) for the thermal camera flight. Background is Mt. Ontake emitting volcanic plume

in a compact size that fits beneath the head part of the UAV. For safe flight operations in the UAV observations, takeoff decision was made only when the ground-level wind speed was below 5 m/s. During the flights, the UAV was always in radio contact in order to monitor its condition and to secure a return command in case of a trouble or an emergency.

A MultiGAS used during the 2011 Shinmoedake eruption with a fixed-wing UAV (Shinohara 2013) was about 3 kg. Thus, we modified the system to fulfill the requested payload. For SO_2 and H_2S electrochemical sensors and an H_2S semiconductor sensor, we used the same ones as in Shinohara et al. (2011) and Shinohara (2013). For CO_2 and H_2O, a small instrument (TR-76Ui-H, T&D Corp., Japan) including a diffusion-type NDIR CO_2 sensor, a capacitive relative humidity sensor and a platinum resistance thermometer with a data logger was used to minimize the total weight of the system. Absolute H_2O concentration was calculated using the relative humidity and temperature output of the TR-76Ui-H instrument.

A SO_2 scrubber filter was placed in front of the H_2S sensor to avoid the cross-sensitivity for SO_2 as in Shinohara et al. (2011). For SO_2, H_2S and H_2 sensors, the gas was pumped at a rate about 700 mL/min through 0.45-μm membrane filter. These sensors and the pump were powered by a 3S Li-Po 11.1V 360 mAh battery (YT3S20C360, Yuntong Power CO. Ltd., China), and output voltages of the sensors were logged every second with a data logger (MCR-4V, T&D Corp., Japan). All instruments were packed into a 236 mm × 164 mm × 110 mm lightweight plastic box attached to the bottom of the UAV except for the TR-76Ui-H instrument that was attached to outside the box (Fig. 2a). The total weight of the system including the box was ~1300 g.

The miniature UV spectrometer system for DOAS measurements was similar to those used in elsewhere (e.g., Galle et al. 2003; Mori et al. 2007; Mori and Kato 2013) and consisted of a miniature spectrometer (USB2000+, Ocean Optics Inc., the USA), a 20-cm-long optical fiber (ϕ = 600 μm), a collimator lens with a visible light cut filter (U-330, Hoya Corp, Japan), a one-board tiny computer (Raspberry Pi Model B+, Raspberry Pi Found., UK) and a mobile battery (5 V output with 6000 mAh@3.7 V). The Raspberry Pi PC runs with Linux-based OS, and observation program was implemented with Python language to automatically control the spectrometer and record the spectrum into a 32 GB SD card memory. The collimator lens was attached to the arm of the multirotor drone to aim upward during the flights, and the rests were packed into a plastic box (175 mm × 140 mm × 75 mm). The total weight of the instrument was about 900 g.

The infrared thermal imaging camera (InfReC G120EX, Nippon Avionics Co. Ltd., Japan) has 320 × 240 pixels with a field of view of 32° by 24° and has a 2 Megapixels CMOS camera for simultaneous visible images. It was attached to the bottom of the UAV with a nadir angle of 30°. The thermal imaging camera records up to the 8000 images into a SD card memory. Operator cannot remotely adjust camera settings including a temperature range, a focus and a sampling rate during its flights. We fixed a temperature range of −40 to 120 °C with a resolution of 14 bit. A focus of the thermal camera was set to an optimal value, which corresponds to a length between the main vent and positions of the UAV. In November 2014 campaigns, thermal images were recorded every 3 s because it is minimum intervals to get visible images simultaneously. The thermal camera is capable of recording images with a sampling rate of 1–10 Hz without visible image recording. In June 2015 campaign, we recorded thermal images every 1 s, whereas visible images were taken by a fish-eye camera (Pixpro SP360, Kodak Inc.) attached to the thermal camera. The weight of the thermal imaging camera is about 800 g, which includes lithium-ion battery pack.

For in-plume particle sampling, an adhesive sheet-type dust sampler (DS-20, NTT-AT Creative Corp., Japan) was used by attaching to the body or the instrument boxes during the flights (Fig. 2a). The sheet was later checked with microscope for investigation of particles on the sheet.

Results

Three UAV measurement campaigns were carried out on November 20 and 21, 2014, and June 2, 2015. Taking off and landing points were selected as shown in Fig. 1b for the respective campaigns considering availabilities, safety issues and wind directions. The distances and azimuth directions of the points from the summit Kengamine peak were 2.9 km (74°), 3.0 km (142°) and 2.3 km (138°), respectively, for points A, B and C in Fig. 1. Altitudes of the points A, B and C were 2135, 2178 and 2234 m, respectively. We made one SO_2 flux flight and one MultiGAS flight on 20 November; one SO_2 flux flight, two MultiGAS flights and one thermal camera flight on 21 November; and two SO_2 flux flights, two MultiGAS flights and one thermal camera flight on 2 June. Figures 3 and 4 show flight routes for November 2014 and June 2015 campaigns, respectively. Red and blue lines correspond to traverse routes for SO_2 flux measurements, which flew under the plume at the altitude of about 2600 m in November 2014 and about 2830–2930 m in June 2015. Green and orange flight routes are for

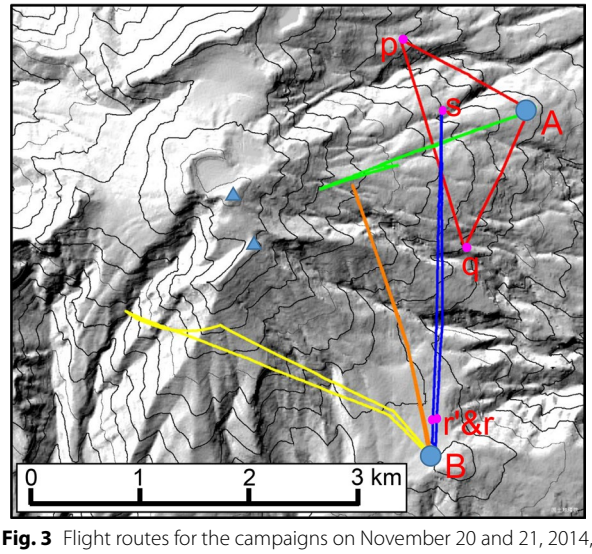

Fig. 3 Flight routes for the campaigns on November 20 and 21, 2014, plotted in the same map as in Fig. 1b. See text for details. Points *p–s* are position corresponding to the respective times during the SO_2 flux flights in Fig. 5a, b. *Solid circles A* and *B* correspond to taking off and landing points in Fig. 1b

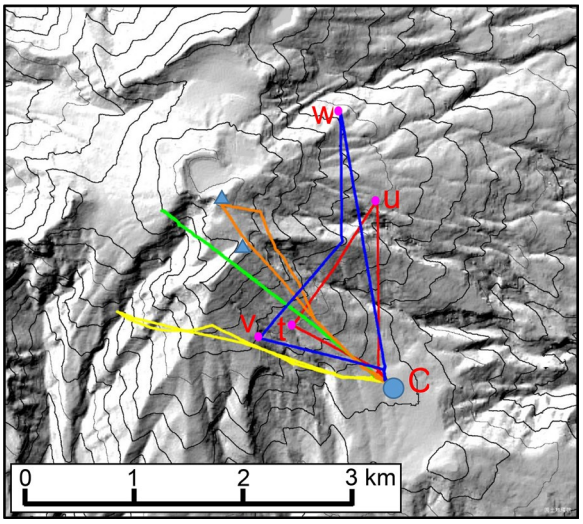

Fig. 4 Flight routes for the campaign on June 2, 2015, plotted in the same map as in Fig. 1b. See text for details. Points *t–w* correspond to the data points on the time series plots of SO_2 flux in Fig. 5c, d. A *solid circle C* corresponds to taking off and landing points in Fig. 1b

MultiGAS flights, which were aimed to enter the plume. Orange lines in the figures correspond to two flights with almost identical horizontal route but with different altitudes. Yellow routes in the figures are temperature measurement flights by the thermal imaging camera. In the MultiGAS flights, the dust sampler sheets were attached either on the body of the UAV or on the instrument box for particle sampling.

SO_2 flux measurements by the UAV

On 20 November, plume was moving toward ENE direction; thus, the taking off and landing point A was used on the day because it was under the plume. The traverse route was in a triangle shape (red line in Fig. 3). Figure 5a shows SO_2 column amount during the traverse. Locations of the UAV at times **p** and **q** in the graph correspond to the respective points in Fig. 3. On 21 November, plume was flowing toward east and the point B was selected as the taking off and landing points considering the thermal camera flight and wind direction. The traverse route corresponds to the blue line in Fig. 3. Figure 5b shows SO_2 column amount during the traverses. Locations of the UAV at times **r**, **s**, and **r'** correspond to the respective points in Fig. 3. In the flux calculations, wind speed from grid point value (GPV) data for 700 hPa (about 3000 m a.s.l.) estimated from numerical weather prediction by JMA was used as the plume speed (data were provided by JMA). The fluxes obtained for 20 and 21 November campaigns were 140 and 130 t/d, respectively (Table 1). Car traverse measurements that were carried out by JMA about 10 km downwind from the summit on 20 November showed fluxes of 100–200 t/d. Our result was within the range of the fluxes obtained by JMA. In the flux measurements, the biggest source of the error is often the plume speed (Stoiber et al. 1983; Mather et al. 2006). In the detailed error estimation of Galle et al. (2010), they categorized measurement conditions as "Good," "Fair" and "Bad," and estimated errors for "Good" and "Fair" conditions were 26 and 54 %, respectively. The conditions of our UAV campaigns corresponded to "Good," and thus, we considered that the error for the above fluxes was around 26 % level.

Figure 5c, d shows SO_2 column amount variation during the traverses on June 2, 2015. The plume was flowing basically toward east on the day, and the point C in Fig. 1 was used for the taking off and landing location. Figure 5c corresponds to the red line flight route in Fig. 4; SO_2 column amount during the flight was mostly negligible, and peaks at time **t**, **u** and afterward correspond to saturation of spectrometer due to the direct sunlight. Especially after time **u** heading back south toward the point C, the spectrometer was mostly saturated due to the slight tilt of the UAV toward the south, which made the sun come in the field of view of the spectrometer. In the second SO_2 flux flight (blue line in Fig. 4), the flight route was extended more to the north to confirm that the traverse went completely under the plume. As shown in Fig. 5d, SO_2 column amounts are in the background level throughout the flight. Two peaks at around 16:32 correspond to SO_2 cells with 94 and 194 ppmm. Times range **v**–**w** and **w**-16:30 in Fig. 5d correspond to northward and southward traverse below the plume; however, there is no clear signal of SO_2 during the periods. From these results, SO_2 flux on June 2, 2015, was under detection limit of the instrument used. In order to see the conditions of the plume, we attached a fish-eye camera (Pixpro SP360, Kodak Inc.) to the UAV in some of the flights in June 2015 campaign. In the green line flight route in Fig. 4 for the MultiGAS flight, the camera was put beneath the UAV. A photograph taken from NW edge of the flight route at an altitude of about 3285 m (Fig. 6) shows that the plume was flowing straight toward east between Kengamine and

(See figure on next page.)

Fig. 5 Sulfur dioxide column amount change with time during the SO_2 flux flights; **a** on November 20, 2014 (*red line* in Fig. 3), **b** on November 21, 2014 (*blue line* in Fig. 3), **c** on June 2, 2015 (*red line* in Fig. 4) and **d** on June 2, 2015 (*blue line* in Fig. 4). Times *p–w* in the plots correspond to the respective positions in Figs. 3 and 4

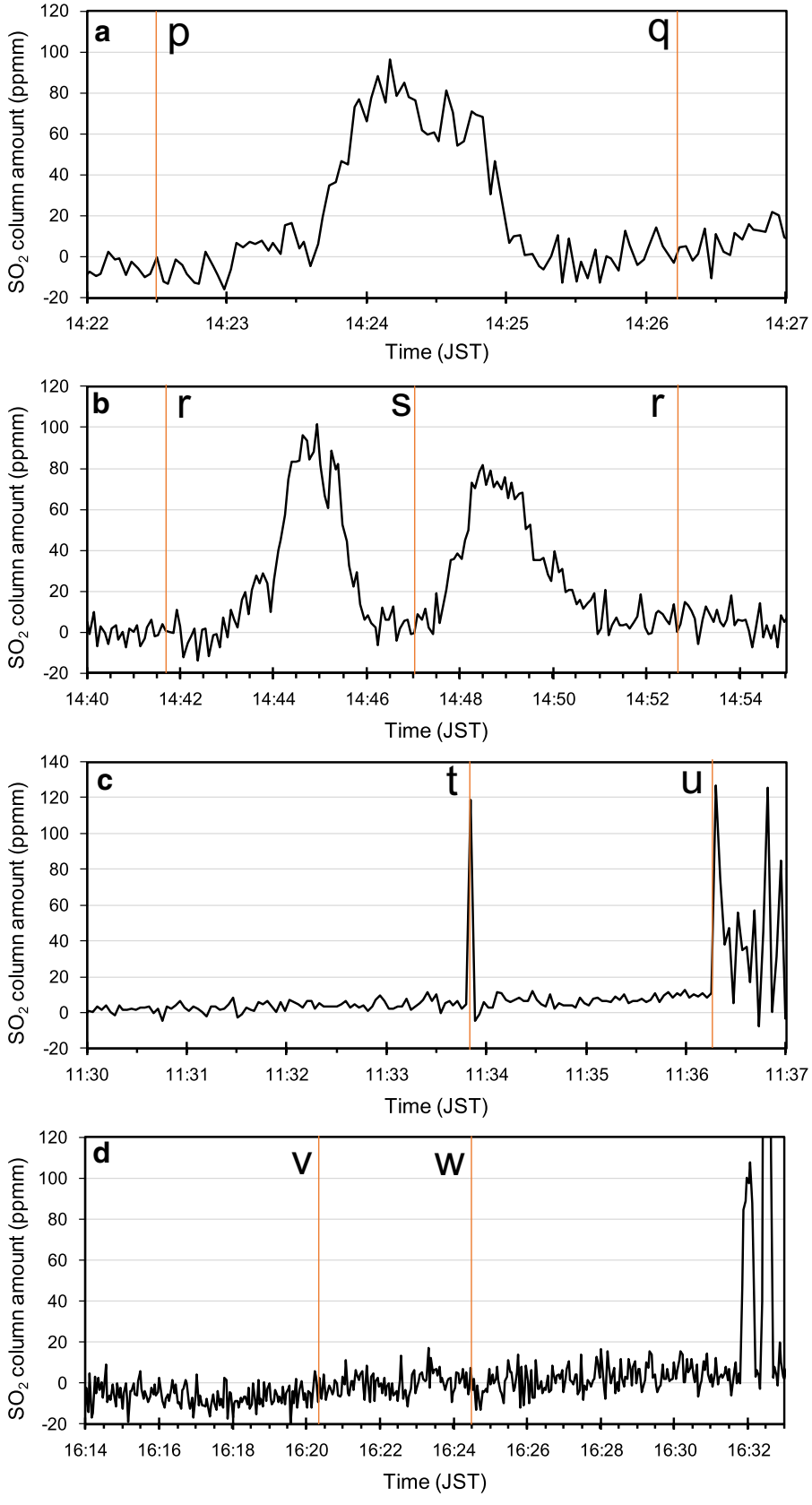
a
p
q
SO2 column amount (ppmm)
120
100
80
60
40
20
0
-20
14:22
14:23
14:24
14:25
14:26
14:27
Time (JST)
b
r
s
r
SO2 column amount (ppmm)
14:40
14:42
14:44
14:46
14:48
14:50
14:52
14:54
Time (JST)
c
t
u
SO2 column amount (ppmm)
140
120
100
80
60
40
20
0
-20
11:30
11:31
11:32
11:33
11:34
11:35
11:36
11:37
Time (JST)
d
v
w
SO2 column amount (ppmm)
16:14
16:16
16:18
16:20
16:22
16:24
16:26
16:28
16:30
16:32
Time (JST)

Table 1 Results of plume measurements at Mt. Ontake

Date	SO_2 flux (t/d)	Traverse method	SO_2/H_2S molar ratio	Flight method	H_2S flux (t/d)	S flux (t/d)
October 09, 2014	450[a]	car	0.31	Helicopter[c]	770	950
November 20, 2014	140	UAV	0.093	UAV	800	820
November 21, 2014	130	UAV	0.097	UAV	710	730
March 26, 2015		car	0.04	Cessna[d]		
June 02, 2015	<7[b]	UAV	0.034	UAV	<110	<110

[a] 400–500 t/d measured by JMA on October 9, 2014 (JMA 2014b)

[b] The value is the maximum estimate. See text for details

[c] Measured by RK by a manned helicopter

[d] Measured by AT by a manned Cessna aircraft

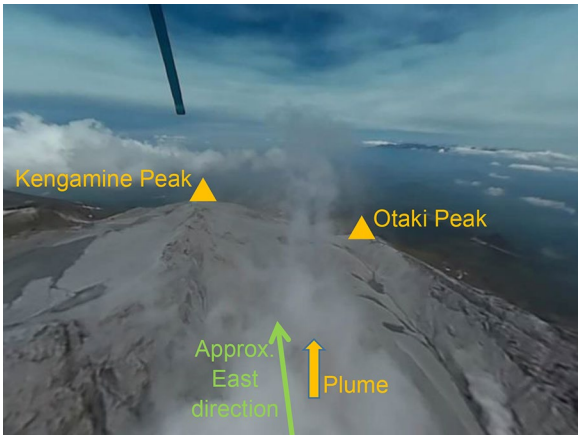

Fig. 6 Summit area and the plume photographed in the air (3285 m) during one of the MultiGAS flight in June 2015 at the NW edge of the *green line* in Fig. 4. The image was taken by the camera onboard the UAV, looking down approximately toward the east. *Two triangles* on the *left* and *right* correspond to Kengamine and Otaki Peaks, respectively. The plume was flowing down approximately eastward as indicated with *orange arrow*

Otaki peaks (much closer to Otaki peak) (Fig. 1b), implying that both traverses crossed the plume on 2 June. During the red line traverse flight in Fig. 4, the camera was attached on top of the UAV. The images clearly showed that the traverse completely passed under the plume.

From these evidences, we confirmed that our flight routes were appropriate for the traverse measurements. Considering the noise level in Fig. 5c and taking an undoubtedly overestimated value (10 m/s) for the wind speed during the traverse (red line in Fig. 4), the SO_2 flux on the day should not exceed 7 t/d (Table 1).

MultiGAS measurements with the UAV

The green line in Fig. 3 indicates the flight route for the MultiGAS measurement on 20 November heading straight toward the summit direction from the point A up to the height of 3300 m (Fig. 7a2). Figure 7a1 and a2 shows SO_2 and H_2S concentrations and corresponding height of the UAV during the flight, respectively. The concentrations in the figure are calculated from raw voltage output using offsets and calibration factors. All the concentration data in our results are pressure-corrected based on the altitude from the flight data. Since the scale of H_2S is an order of magnitude larger in the plot, it is clear that H_2S is the major sulfur-bearing gas species. Significant noises in SO_2 concentration are due to electrical noise probably from motors of the UAV (Fig. 7a1). The noise becomes significant during ascent and descent of the UAV when the motors are in high rotation. Similar noise is also slightly visible in H_2S concentrations. In order to diminish the noise, we taped aluminum sheets all inside the instrument box of MultiGAS for electromagnetic shielding. As shown in Figs. 7b1, c1 and d1, the noise is substantially reduced in the following measurements in Fig. 7d1.

Figure 7b1, c1 shows SO_2 and H_2S concentrations of the two flights carried out on 21 November. The flight routes are horizontally identical in the plan view (orange line in Fig. 3) but slightly different in altitude (Fig. 7b2, c2). The peak concentrations of H_2S and SO_2 were about 4 ppm and 0.4 ppm, respectively, for the two flights. For the second MultiGAS flight on 21 November, CO_2, H_2O, H_2 concentrations and temperature during the flight are plotted, respectively, in Fig. 7c3, c4, c5 and c6. Two MultiGAS flights were done on June 2, 2015. However, the former flight (the green line in Fig. 4) seemed to pass over the plume and did not detect any volcanic gas. Thus, the result of the latter flight (the orange line in Fig. 4) is presented here (Fig. 7d1, d2). The highest H_2S value of 10.5 ppm was recorded during the flight. Considering the response time of about 30 s for the sensors (Shinohara et al. 2011), real concentration in the plume was likely to be much higher.

Molar ratios of SO_2 over H_2S for all the flights were calculated from correlation plots as in previous MultiGAS

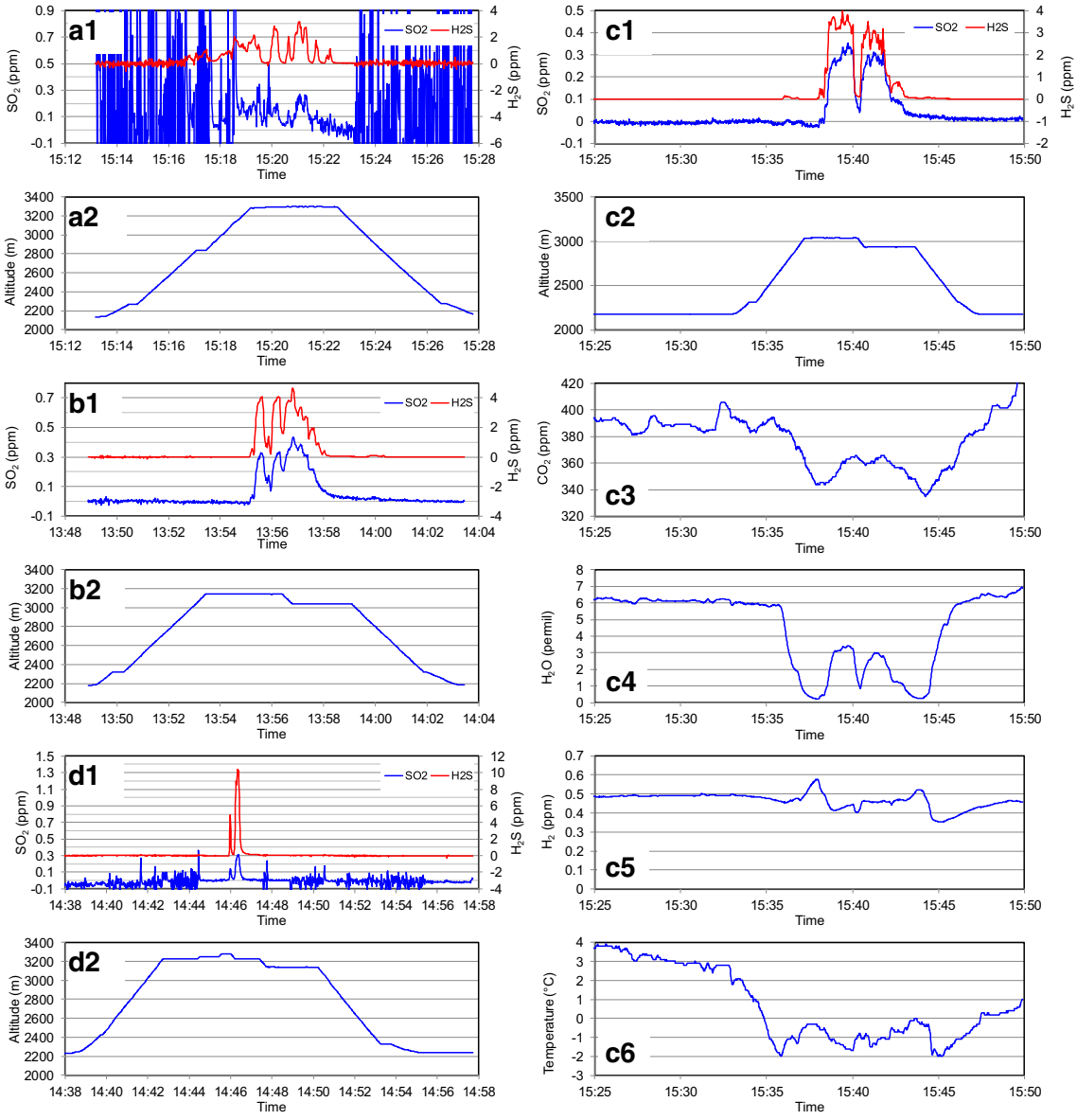

Fig. 7 Plots showing temporal variations of SO_2 and H_2S concentrations (**a1**, **b1**, **c1** and **d1**) and flight altitude (**a2**, **b2**, **c2** and **d2**) during the MultiGAS flights in Figs. 3 and 4; (series a) on November 20, 2014 (*green line* in Fig. 3). (series b) and (series c) for the first and the second flights on November 21, 2014 (*orange line* in Fig. 3). (series d) on June 2, 2015 (*orange line* in Fig. 4). For the second MultiGAS flight, temporal variations of CO_2, H_2O, H_2 concentrations and temperature are plotted, respectively, in c3–c6

studies (Shinohara 2005, 2013; Shinohara et al. 2011; Aiuppa et al. 2005a, b). Figure 8a–d shows SO_2 versus H_2S scatter plots of the four MultiGAS flights. The original concentration time series data in Fig. 7 were moving averaged for 1 min to make apparent response times common to the two sensors and then were shifted in time axis to adjust the lags between them. The slopes of the regression lines correspond to SO_2/H_2S molar ratios in the plume. As shown in Fig. 8, determination coefficients were high implying very homogeneous mixing inside the plume. The estimated SO_2/H_2S molar ratios are 0.093, 0.097 (an average of the two flights) and 0.034, respectively, for November 20 and 21, 2014, and June 2, 2015, campaigns (Table 1). Considering the errors in calibration and background (zero level) variations, the estimated errors for the ratios are about 7 %.

Our MultiGAS had also CO_2, humidity (H_2O) and H_2 sensors. Figure 7c3–c5 shows CO_2, H_2O and H_2

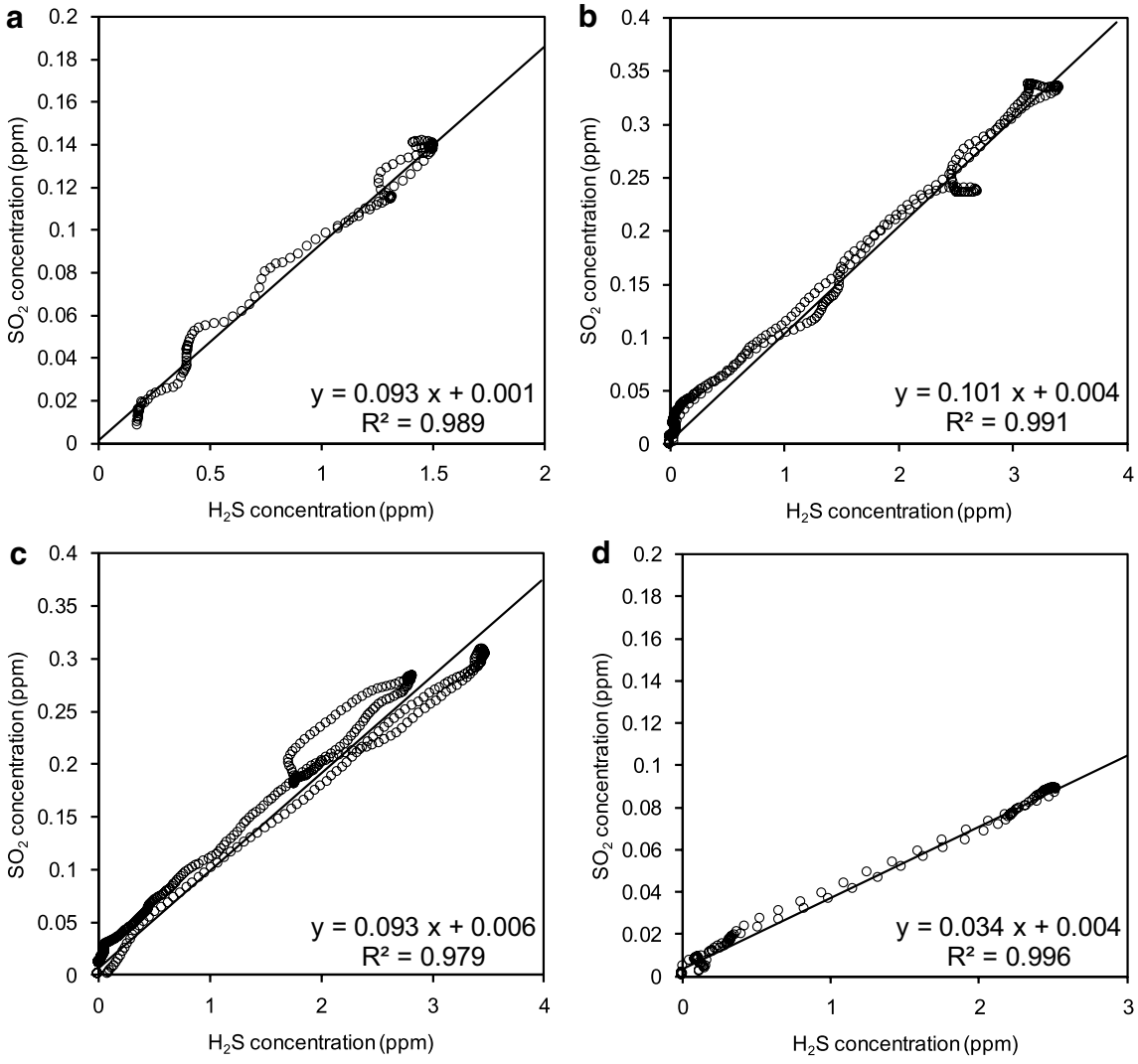

Fig. 8 Scatter plots of H_2S and SO_2 concentrations showing correlations for MultiGAS flights measurements; (**a**) on November 20, 2014, (**b**, **c**) on November 21, 2014, and (**d**) on June 2, 2015. For plot (**a**), data between 15:20:30 and 15:22:40 were used to minimize the influence of electrical noise from the motors in the SO_2 trace (Fig. 7a1). The equations and R^2 values on the *right bottom* of each panel are linear regression lines and coefficients of determination, respectively

concentrations observed during the second MultiGAS flight on 21 November. The CO_2 and H_2O sensors in TR-76Ui-H instrument have slower time responses than those for the SO_2 and H_2S sensors. We can clearly recognize increase in CO_2 (Fig. 7c3) and H_2O (Fig. 7c4) concentrations with SO_2 and H_2S concentrations (Fig. 7c1), but we cannot see a similar variation on the H_2 data (Fig. 7c5). Scatter plots for H_2O and CO_2 against H_2S concentrations in Fig. 9 show linear trends as if the H_2O/H_2S and CO_2/H_2S molar ratios are 820 and 6.0, respectively. However, these ratios are most likely to be affected severely by entrainment of the ambient air at low altitude with high H_2O and CO_2 concentrations observed during the measurement (Fig. 7c3, c4) and do not simply reflect volcanic gas composition. Both CO_2 and H_2O concentrations were high at the ground level and started to decrease at around 15:36 coinciding with the local minimum of the atmospheric temperature (Fig. 7c6). This implies the existence of a thermal inversion around 2700 m a.s.l. and that the upper layer was poorer in CO_2 and H_2O than the lower layer.

Ratios between volcanic gas species are estimated using the scatter plot with an assumption of two-component mixing of a volcanic gas and an atmosphere with a fixed composition. The linear trends on Fig. 9 indicate such simple two-component mixing. However, the volcanic

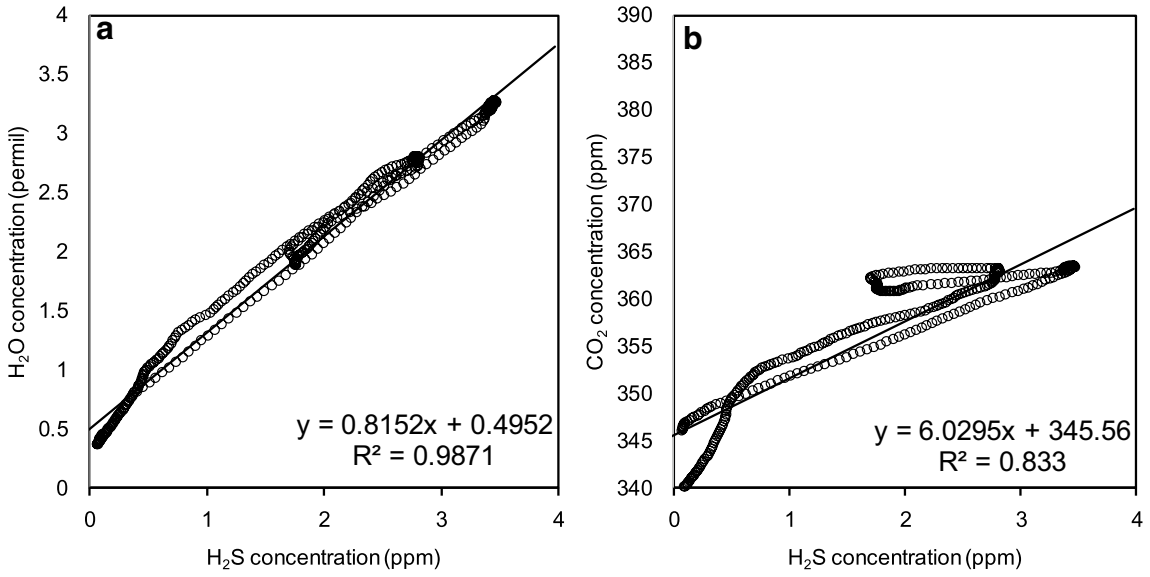

Fig. 9 Scatter plots of H_2O (in permil) and CO_2 against H_2S concentrations showing correlations for the second MultiGAS flights on November 21, 2014. Data between 15:27:45 and 15:43:30 were used to select the period during which the UAV was flying horizontally at altitudes between 2930 and 3040 m. The equations and R^2 values on the *right bottom* are linear regression line and coefficients of determination, respectively

gases that have left the vents at around 2800 m a.s.l. ascend to ca. 3000 m as a plume, entraining the ambient air at various altitudes in the course of the ascent. The volcanic plume measured by the UAV is not a simple mixture of the volcanic gas and the atmosphere at 3000 m a.s.l. but also contain the lower altitude atmosphere. The linear trends in Fig. 9 are likely caused by mixing of the atmosphere at 3000 m a.s.l. and the volcanic plume that has entrained the lower altitude atmosphere in the course of the ascent.

We demonstrate the effect of entrainment of the low altitude atmosphere with different compositions with a simplified example of the following two-step air-mixing model. At the first step, the volcanic gas is assumed to be diluted to $H_2S = 5$ ppm with the low altitude atmosphere at 2,800 m a.s.l. of $H_2O = 4.5$ permil and $CO_2 = 375$ ppm and forms a plume of $H_2O = 4.5$ permil, $CO_2 = 375$ ppm and $H_2S = 5$ ppm. Here, we neglect H_2O and CO_2 concentrations in volcanic gas as an extreme example to simply explain what we have observed. During ascent, the plume will be homogenized by turbulence, and then, the homogeneous plume is mixed with the atmosphere at 3000 m a.s.l. where atmospheric composition is $H_2O = 0.5$ permil and $CO_2 = 345$ ppm. The results of an airborne measurement at this height will be plotted along a linear mixing line between the plume from 2800 m a.s.l. and the atmosphere at 3000 m a.s.l., such as shown in Fig. 9. This example shows that sequential entrainment of atmospheres with different compositions can produce mixing line similar to that by mixing of the uniform atmosphere and volcanic gas even in the extreme case that volcanic H_2O and CO_2 are not considered. We cannot see the effect of the lower altitude atmosphere on the scatter plots because turbulence in the ascending plume well mixes the volcanic gas and the low altitude atmosphere before mixing with the high altitude atmosphere. Further evaluation of this air entrainment process is not possible, because air entrainment factor as a function of altitude is not known. We conclude that we cannot estimate volcanic H_2O/H_2S and CO_2/H_2S ratios with these results.

Detailed assessment of this problem is not the scope of this study, but our results clearly show that this problem is very serious for volcanic plume chemistry measurements using the MultiGAS. In the MultiGAS measurements, a constant atmospheric composition is implicitly assumed for estimating concentration ratios of volcanic gas species. For gas species common in both volcanic gas and atmosphere such as CO_2 and H_2O, difference in ambient air compositions near the vent and at observation site causes over estimation of volcanic gas ratios at one time but does under estimation at other times. This problem is negligible for volcanic gas ratios between gas species, which have ignorable amount in the atmosphere such as SO_2, H_2S and HCl.

Thermal camera observations

Thermal and visible images were automatically recorded on the scheduled flight route (yellow lines in Figs. 3 and 4) at a speed of 5–6 m/s. Horizontal distance from the

main vent during measurements was set to approximately 900 m because a focus of the thermal camera was fixed. A spatial resolution around the main vent was 1.8 m × 1.8 m/pixel, which was sufficiently smaller than the vent diameter of several tens of meters.

In November 21, 2014, campaign, the main vent was photographed in about 100 thermal and visible images. The maximum temperature of 90.6 °C was found around the main vent from which volcanic gas ejected vigorously (Fig. 10a). The temperature was comparable to the boiling point at the altitude of the main vent. In June 2015 campaign, the main vent was photographed in 260 thermal images. The maximum temperature around the main vent was 101.9 °C (Fig. 10b).

In-plume particle sampling

In some of the flights on November 21, 2014, and June 2, 2015, some adhesive sheets were attached to the UAV's head for the purpose of sampling fine particles floating in the air. Under microscope observation, we identified 3–50 particles per 100 cm^2 with diameters between 0.05 and 0.4 mm. However, we also identified similar particles even for the flights outside the plume, and no meaningful difference was observed regardless of plume entry. We thus consider that the particles were not from the plume but were probably wound up by the wind from the ground.

Other observations

Apart from the UAV measurements, our group had conducted several other volcanic plume observations for the 2014 eruption of Mt. Ontake. We carried out two MultiGAS measurements with a manned aircraft on October 9, 2014, 2 weeks after the onset of the phreatic eruption, and on March 26, 2015. The former measurements were done onboard the helicopter flown by Japan Ground Self-Defense Force. Since the helicopter could just glanced the edge of the plume, only the measurements of the SO_2/H_2S molar ratio, showing 0.31, was reliable. The latter observation was carried out by a fixed-wing aircraft on March 26, 2015, during the thermal camera observation. H_2S concentration was of the order of 1 ppm, while SO_2 concentration was 0.03–0.05 ppm. For the ratio estimation, peak heights are compared instead of using the correlation on a scatter plot. Because of the low SO_2 concentration close to the noise level, the estimated ratio was 0.04 with the error of 30–50 %.

Figure 11 shows the change in molar ratio of the SO_2/H_2S after the 2014 eruption. We also plotted together the ratios after the 1979 eruption using the data of Ossaka et al. (1983) and Sugiura et al. (1997) for comparison.

Sulfur dioxide flux measurements were repeated after the eruption using a compact UV spectrometer system (COMPUSS; Mori et al. 2007) with car traverses by JMA. The SO_2 flux ranged over 700–1300 t/d for the first week after the eruption and gradually decreased from 500 t/d level to 100–200 t/d by the end of October (JMA 2014b). Our group also carried out car traverse measurements for the first several days. Our first measurement was carried out at 9:00 (JST) on September 28, which recorded 2500 t/d, before the measurements by JMA started. The SO_2 flux gradually decreased down to about 400 t/d by 14:00 (JST) on the day. The result shows that the volcano had very high flux at least

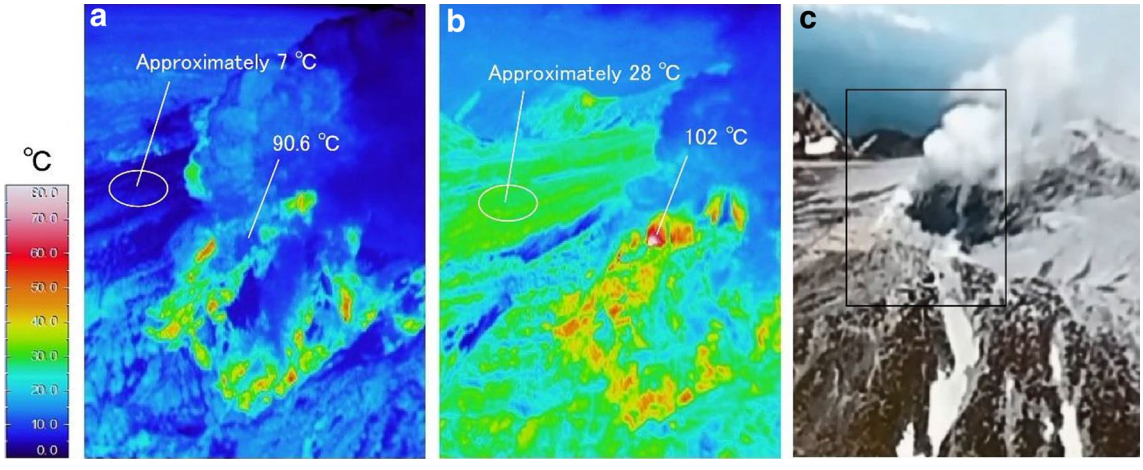

Fig. 10 Thermal images of the vent area in Jigokudani observed during the UAV flights on November 21, 2014, (**a**) and on June 2, 2015 (**b**). The temperature *color scale* is indicated on the *left*. The white ellipse in (**a**) and (**b**) indicates the background temperature of each day. Locations of the maximum temperatures are also indicated. (**c**) is a visible image of the summit area. The inset corresponds to the viewing field of the thermal images (**a**) and (**b**)

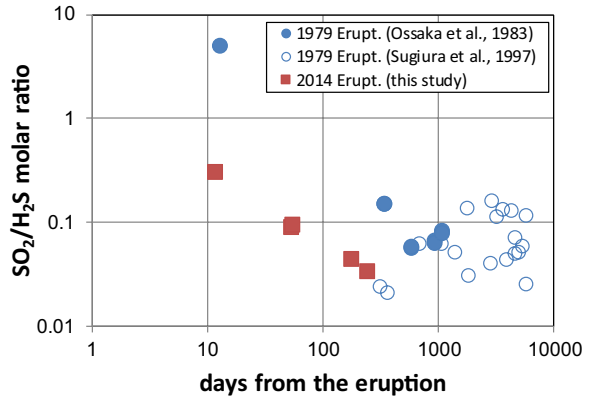

Fig. 11 Temporal variation of SO_2/H_2S ratio after the 2015 eruption (*solid squares*). The variation for the 1979 eruption is also plotted for comparison using the data from Ossaka et al. (1983) (*solid circle*) and Sugiura et al. (1997) (*open circle*)

within a day of the onset of the eruption on September 27, 2014.

Three thermal camera observations were carried out with a helicopter and a light airplane. On October 16, 2014, a helicopter operated by the Mainichi Newspaper approached 1500 m distance from the main vent. The maximum temperature was found to be 60 °C. However, visibility was poor because Jigokudani area was covered with fumarolic gas. Second and third observations were carried out by a fixed-wing airplane on October 25, 2014, and March 26, 2015, respectively. At the former observation, we recorded thermal images from 3000 m distance over the main vent. The maximum temperature around the main vent was 80.6 °C. The latter observation was carried out at the distance of about 2400 m from the vents; however, the main vent was not clearly observed due to dense fumarolic plume.

Discussion and conclusions

Advantages and potentials of the UAV measurements for volcanic plume observation have already been clear from previous studies (e.g., McGonigle et al. 2008; Shinohara 2013). In particular, application of UAVs to ongoing eruptions like in Shinohara (2013) has great merit from the standpoint of safety and practicality. Our study has proven that multirotor UAVs are capable of in-plume measurements at an altitude over 3000 m a.s.l. Since Mt. Ontake is the second highest volcano in Japan, we are now confident that such UAVs are applicable for most volcanoes in Japan if once we can approach at least to 3 km from the target area. Although this clearance is usually a safe distance, it would easily be extended in the near future by improvement of batteries and the UAVs themselves.

Regarding SO_2 flux measurements, the use of the UAVs is not always necessary when the flux is substantial and a subaerial traverse route is close enough to the target plume to detect measurable SO_2 column amount of at least a few tens of ppmm as the peak amount. In the particular case of Mt. Ontake with a huge volcanic edifice, however, roads for car traverse measurements are not available within 10 km from the main vents. The car traverse measurements conducted by JMA on November 20, 2014, recorded only 30 ppmm even just under the plume center (pers. Comm. Koji Kato of JMA), whereas our UAV measurements with a clearance about 2 km on the same day recorded ca. 100 ppmm. The UAV traverse measurements are not restricted by the presence of adequate roads like in the case of car traverse, and thus, routes design can be flexible; in principle, even traversing the very vicinity of the plume vents is possible. This technique has significant advantage for the volcanoes with very low flux, especially in a waning period of an eruption. Considering the safety, simplicity and relatively lower cost compared to manned aircrafts, measurements with multirotor drone UAVs will soon be further more useful in many situations of volcanological interest.

Volcanic gas fluxes are in general measured using UV spectroscopic methods for SO_2 because of negligible atmospheric abundance and spectroscopically detectable absorption features of the species in the plume (e.g., Oppenheimer 2010). Thus, SO_2 has been the key species for gas flux measurements of the volcanic plumes. In contrast, H_2S, another major sulfur volcanic gas species, has not yet successfully been monitored by remote flux measurements. In order to retrieve H_2S flux in a plume, two types of methods have been used in volcanic surveys. One is a combination of SO_2 flux and SO_2/H_2S ratio in a plume (e.g., Bandy et al. 1982; Aiuppa et al. 2005a, b) and the other is the H_2S concentration profiling for a plume cross section by an aircraft for huge plumes (e.g., Radke et al. 1976; McGee et al. 2001) or by walk for small plumes (Allard et al. 2014). Unlike the remote sensing for SO_2 flux measurements, both the above methods need to bring sensors into a plume. The former method is only applicable when the SO_2 flux can be constrained by spectroscopic method and is usually impossible for low-temperature fumaroles with low SO_2 and predominant H_2S (Allard et al. 2014). These are the reasons that number of reported H_2S fluxes for volcanoes are limited compared to that for SO_2 fluxes (McGee et al. 2001; Aiuppa et al. 2005a, b). In this study, the former method was applied because SO_2 flux was measurable at least for the UAV campaign in November 2014. Considering the inaccessibility of the summit area due to severe winter condition and a risk of flying manned aircraft into the plumes, the use of the UAVs deserved H_2S flux quantification for Mt.

Ontake. Further, we consider this method can be applied to any other volcanoes emitting measurable SO_2 flux. Meanwhile, the plume profiling, the latter method, may be applicable by using the UAVs for relatively small-sized plumes but probably still difficult for huge plumes that need to fly long distances.

Table 2 shows reported H_2S fluxes with information of methodology and major S species in the plume for various volcanoes. Major sulfur species for the most of the volcanoes in the list is SO_2, and thus, the measured values are mostly corresponding to magmatic gas compositions. The number of volcanoes that has H_2S flux over 500 t/d is limited, and reported fluxes for most volcanoes are below several tens t/d (Table 2). Even one of the strongest SO_2 emitters, Mt. Etna (e.g., Oppenheimer et al. 2011), discharges H_2S only up to 50 t/d. The highest H_2S flux reported is for Mt. St. Helens, which emitted 8600 t/d during a paroxysmal eruption on May 18, 1980 (Hobbs et al. 1981, 1982). The 1980–1981 eruption of Mt. St. Helens was exceptional, and high H_2S flux exceeding 800 t/d was reported even in the post-eruptive period (Hobbs et al. 1982). The other high H_2S flux over 1000 t/d was reported Redoubt Volcano during 2009–2010 (Werner et al. 2013). The highest flux of 1230 t/d was reported during magmatic eruption when simultaneous SO_2 flux was over 10000 t/d (Werner et al. 2013). The two highest fluxes in Table 2 were observed for eruptive activities, and those were accompanied by much larger-scale eruptions compared to that of the 2014 eruption of Mt. Ontake. Except for the unusual eruptive activities of Mt. St. Helens, Mt. Ontake emitted very high H_2S flux for the plume probably influenced by hydrothermal system. Considering the SO_2 flux decrease from 450 t/d to about 130 t/d and the SO_2/H_2S molar ratio change from 0.31 to about 0.1 for Mt. Ontake from 2 weeks after to 2 months after the eruption (Table 1), it is likely that the volcano had kept H_2S flux of 700–800 t/d at least for about 2 months. This amount of H_2S is not negligible for the S budget at volcanoes. The eruption of Mt. Ontake reaffirmed the significance of H_2S emission from volcanoes and implying the importance of monitoring H_2S flux for phreatic

Table 2 Reported H_2S emission rates from volcanoes

Volcano	Period	H_2S flux (t/d)	Major sulfur[c]	Method[d]	References
Mt. Baker	1975, 2000	5.5–112	H_2S	C. D.	Radke et al. (1976), McGee et al. (2001)
Mt. St. Helens (phreatic period)	March–May 1980	2.6–43	H_2S	C. D.	Hobbs et al. (1982)
Mt. St. Helens (IE & P[a])	May–June 1980	260–8600	H_2S	C. D.	Hobbs et al. (1982)
Mt. St. Helens (PE[b])	June 1980–June 1981	1.7–864	SO_2	C. D.	Hobbs et al. (1982)
Mt. St. Helens (PE[b])	September 1980	65	SO_2	Ratio	Bandy et al. (1982)
White Island	2004, 2005, 2006	2–19	SO_2	C. D.	Werner et al. (2008)
Redoubt	2009, 2010	1–1230	SO_2	C. D.	Werner et al. (2013)
Redoubt	1997, 2000, 2001 2005	0–1	SO_2	C. D.	Doukas and McGee (2007)
Spurr	2004	0.2–3	H_2S	C. D.	Doukas and McGee (2007)
Spurr	2005, 2006	0–6.7	SO_2	C. D.	Doukas and McGee (2007)
Iliamna	2001–2005	0–4	SO_2	C. D.	Doukas and McGee (2007)
Augustine	2002–2006	0–8.2	SO_2	C. D.	Doukas and McGee (2007)
Fourpeaked	2006	27–140	SO_2	C. D.	Doukas and McGee (2007)
Mageik	2004	69	H_2S	C. D.	Doukas and McGee (2007)
Martin	2002, 2004	0–43	SO_2	C. D.	Doukas and McGee (2007)
Etna	1978, 1979	1–10	SO_2	C. D.	Jaeschke et al. (1982)
Etna	2003	50	SO_2	Ratio	Aiuppa et al. (2005a, b)
Stromboli	2003	8	SO_2	Ratio	Aiuppa et al. (2005a, b)
Vulcano	2003	6	SO_2	Ratio	Aiuppa et al. (2005a, b)
Bromo	2014	17–25	SO_2	Ratio	Aiuppa et al. (2015)
La Soufriere	2006, 2012	1–3.8	H_2S	C. D.	Allard et al. (2014)
Mt. Ontake	Oct. & Nov. 2014	710–800	H_2S	Ratio	This study
Mt. Ontake	Jun. 2015	<110	H_2S	Ratio	This study

[a] IE&P: Intra-eruptive and paroxysmal periods

[b] PE: Post-eruptive period

[c] Major Sulfur: Major sulfur species in volcanic plume

[d] Method: Methods for H_2S flux measurement. C. D.: concentration distribution by profiling; Ratio: combination SO_2 flux and SO_2/H_2S ratio

eruption plumes, which are not accompanied by significant SO_2 emissions.

In addition to the observed high H_2S flux, significantly high SO_2 flux at the early stage of the eruptive period is another distinguishing feature of the 2014 eruption of Mt. Ontake. Sulfur dioxide emission of 500–800 t was first detected by Suomi NPP OMPS data about 2 h after the onset of the eruption (NASA-GSFC and Michigan Tech. Univ. 2014) and 2500 t/d of SO_2 flux at 9:00 (JST) in the morning on September, 27, 2014, about 21 h after the eruption onset.

The SO_2 flux decreased with time but sustained the level over 100 t/d at least until 2 months after the eruption (Table 1). Considering that continued SO_2 flux >100 t/d is the probable indicator of magma degassing (Symonds et al. 2001), magmatic gas influence for the 2014 eruption is highly suggestive. In contrast, the 2014 Mt. Ontake eruption is considered as a phreatic one, as no juvenile magmatic material was found in the volcanic ash (Earthquake Research Institute 2014). In their review of phreatic eruptions, Barberi et al. (1992) grouped the eruption into two categories: "explosions of confined geothermal systems with or without the direct action of magmatic fluids" and "explosions caused by the vaporization of surface fluids percolating into the temporarily plugged hot conduit of an active volcano." Sano et al. (2015) concluded that the 2014 eruption belongs to the former group. The significant SO_2 flux observed implies that the eruption belongs to the former group with direct magmatic fluid.

The 1979 Mt. Ontake eruption is also defined as a phreatic eruption from the composition of ash (Sugiura et al. 1980; Ossaka et al. 1983). For the 1979 eruption, the fumarolic gas from the eruption vents was collected repeatedly in a yearly basis from 2 weeks after the eruption for several years (Ossaka et al. 1983; Sugiura et al. 1997). A reported SO_2/H_2S molar ratio for the summit fumarolic sample 2 weeks after the eruption was 4.9 (Ossaka et al. 1983) and had closer value to SO_2/H_2S molar ratio range of 6.6–25 for the major degassing volcanoes in Japan (Shinohara 2013). Together with high H_2 content in residual gas for the fumarolic samples and high Cl/SO_4 ratio of the water-soluble components of ash leachates, Ossaka et al. (1983) concluded that the 1979 Mt. Ontake eruption was not a normal phreatic eruption but had strong influence of high-temperature magmatic gas from the depth. Thus, strong influence of magmatic fluid at the early stage of the eruptive activity is a common event at least for the two eruptions of Mt. Ontake in 1979 and 2014. Input of magmatic fluid into Mt. Ontake's volcanic system had also been suggested by He isotopic ratios of summit fumaroles and flank hot springs (Sano et al. 1984, 1986). Especially for over 10 years before the 2014 eruption, significant increase in $^3He/^4He$ ratio at hot springs at about 4 km from the summit had been reported and is concluded as precursory increased input of magmatic fluid from the depth (Sano et al. 2015). Supporting evidences for the input of magmatic fluids are also found in seismological studies. A few months before the minor eruption in March 2007, a very-long-period (VLP) volcanic event was detected at the depth of 2.4 km from the summit and was explained as interaction between hydrothermal system and input of magmatic fluid ascended from intruded magma body (Nakamichi et al. 2009). By detailed analyses of seismicity before the 2014 eruption, Kato et al. (2015) considered the VT events occurred in middle September to be due to infiltration of hot fluids, probably magmatic fluid, along small faults beneath hydrothermal system. These geochemical and geophysical evidences suggest magmatic fluid influence to the activities of Mt. Ontake, and it is likely that there was significant magmatic fluid input for the 2014 eruption.

Sulfur dioxide flux rapidly decreased after the eruption, and this trend is similar to decreasing trend of number of VT earthquakes (JMA 2014b). The VT events beneath hydrothermal system decreased in number after the eruption (Kato et al. 2015). Thus, magmatic fluid input from the depth seems to have occurred for a short time before the eruption, and the rapidly decreasing SO_2 flux trend seems to be accounted for by this short-lived input. In contrast, although we have no data of H_2S flux at the onset of the eruption, the H_2S flux sustained high flux of 700–800 t/d at least between 2 weeks and 2 months after the eruption and slowly decreased to <110 t/d by June 2015 (Table 1). Ossaka et al. (1983) proposed a model of gas emission system related to the 1979 eruption with input of high-temperature gas from the depth and dry-out or evaporation of shallower hydrothermal system. The observed decrease in SO_2/H_2S molar ratio (Fig. 11) was attributed to temperature decrease in the high-temperature gas (Ossaka et al. 1983). Since there are no gas flux data for the 1979 eruption, we are not able to compare the gas emitting system based on the flux data. For the gas emission system of the 2014 eruption, we speculate a similar model with magmatic fluid input from the depth that triggered the eruption and sustained evaporation of the hydrothermal system. Sulfur dioxide and H_2S fluxes on October 9, 2014, were 450 and 770 t/d, respectively (Table 1). Excluding the case of Mt. St. Helens during the paroxysmal event (Hobbs et al. 1981, 1982), high H_2S flux over several hundred t/d is measured only when SO_2 flux is over several thousand t/d with probable magmatic gas composition (Hobbs et al. 1982; Werner et al. 2013). Thus, the H_2S fluxes observed at Mt. Ontake are very peculiar. The decrease in the sulfur flux

from October 9 to November 20–21 was not very drastic (<20 %; Table 1), which contrasted to the change in volcanic activity for the same period; the eruptive activity was still in a stage with ash emission on October 9 (until October 10), whereas the style of the eruption has shifted to continuous non-ash plume emission by November 20–21. Instead of attributing the observed SO_2/H_2S molar ratio change to cooling of deep high-temperature gas as in Ossaka et al. (1983), we presume that majority of SO_2 and H_2S were supplied from different sources and were, respectively, from high-temperature magmatic fluid and from hydrothermal system. Thus, the ratio change was attributed to changes in the mixing ratio of the gases from these two sources. This is probably one of the simplest models for the flux changes observed for SO_2 and H_2S for the 2014 eruption. Significant volume of hydrothermal system would be needed to maintain H_2S flux of 700–800 t/d at least for 2 months with dissolved and aqueous H_2S in the hydrothermal water. Instead, if we can assume hydrolysis reaction of accumulated sulfur to H_2S (Oana and Ishikawa 1966; Ellis and Giggenbach 1971) in the hydrothermal system of Mt. Ontake, the volume of the system needed may be drastically decreased. In fact, sustained magmatic fluid supply to the hydrothermal system has been indicated by helium-3 studies (Sano et al. 2015). Sulfur brought by the long-term magmatic fluid supply might be a candidate for such accumulated sulfur in the hydrothermal system.

Comparing SO_2/H_2S molar ratios that were measured 2 weeks after the eruptions for the 2014 and 1979 eruptions, the ratio for the 2014 eruption was more than an order of magnitude lower than that for the 1979 eruption (Fig. 11). By considering two different sources for SO_2 and H_2S as above, the difference of the ratio may be attributed to a difference in mixing ratio of magmatic and hydrothermal gases. Compared to the 2014 eruption, input of the magmatic fluid might be much larger in the 1979 eruption. Alternatively, a size of hydrothermal system might have been smaller in the 1979 eruption compared to that in the 2014 eruption.

Current SO_2/H_2S molar ratio (as of June 2015) below 0.05 has already reached almost the lowest level after the 1979 eruption at which the influence of magmatic fluid became negligible (Fig. 11). Increase in fumarolic temperature is still continuing according to the infrared thermography. After the 1979 eruption, similar increase was also observed for a several years, which was explained as a dry-out process of the conduit (Ossaka et al. 1983) and then changed to decreasing trend (Sugiura et al. 1997). Thus, the temperature increase currently observed does not imply an elevation of the volcanic activity. Considering changes in SO_2/H_2S molar ratios and observed SO_2 and H_2S fluxes (Table 1), we speculate that the current activity of Mt. Ontake would slowly cease with time unless an additional input of the magmatic fluid from the depth would take place.

Abbreviations

a.s.l.: above sea level; DOAS: differential optical absorption spectroscopy; JMA: Japan Meteorological Agency; MultiGAS: multicomponent gas analyzer system; UAV: unmanned aerial vehicle; VERP: Volcano Emissions Research Package.

Authors' contributions

TM carried out the UAV observations, built gas instrumentation, analyzed gas data and drafted the manuscript. TH took the lead in the UAV observations and drafted the manuscript. AT carried out the UAV and Cessna observations, measured and analyzed thermal images and drafted the manuscript. MY carried out the UAV observation and analyzed adsorbed particles. RK carried out the helicopter observation and corrected the manuscript. HS helped the instrumentation of the MultiGAS and corrected the manuscript. RT supported the measurements and helped the instrumentation. All authors read and approved the final manuscript.

Author details

[1] Geochemical Research Center, Graduate School of Science, The University of Tokyo, 7-3-1 Hongo, Bunkyo-ku, Tokyo 113-0033, Japan. [2] Institute of Seismology and Volcanology, Faculty of Science, Hokkaido University, N10W8, Kita-ku, Sapporo 060-0810, Japan. [3] Volcanic Fluid Research Center, Tokyo Institute of Technology, 641-36 Kusatsu, Agatsuma, Gunma 377-1711, Japan. [4] Division of Volcanic Disaster Mitigation Research, Mount Fuji Research Institute, Yamanashi Prefectural Government, 5597-1 Kenmarubi, Kamiyoshida, Fujiyoshida, Yamanashi 403-0005, Japan. [5] Geological Survey of Japan, National Institute of Advanced Industrial Science and Technology, 1-1-1 Higashi, Tsukuba, Ibaraki 305-8567, Japan. [6] Department of Natural History Sciences, Graduate School of Science, Hokkaido University, N10W8, Kita-ku, Sapporo 060-0810, Japan.

Acknowledgements

We thank Otaki Village and Kiso Town for facilitating the UAV observations. We are very grateful to a staff of Tokyo Regional Civil Aviation Bureau, Ministry of Land, Infrastructure, Transport and Tourism for their cooperation in our flights with a relative elevation of more than 250 m. We would also like to acknowledge Dr. Andrew J McGonigle and an anonymous reviewer for constructive comments to improve this manuscript. TM acknowledges Masaaki Morita for help in instrumental and field preparations. TM and HS are grateful to Ms. Masami Someya for instrumental calibrations at the laboratory. This work was supported by JSPS KAKENHI Grant-in-aid for Special Purposes Number 26900002. The UAV observations were conducted as members of The Joint Research Team for the 2014 Mt. Ontake Eruption under JMA.

Competing interests

The authors declare that there are no competing interests.

Received: 30 November 2015 Accepted: 24 February 2016
Published online: 22 March 2016

References

Aiuppa A, Inguaggiato S, McGonigle AJS, O'Dwyer M, Oppenheimer C, Padgett MJ, Rouwet D, Valenza M (2005a) H_2S fluxes from Mt. Etna, Stromboli, and Vulcano (Italy) and implications for the sulfur budget at volcanoes. Gochim Cosmochim Acta 69(7):1861–1871. doi:10.1016/j.gca.2004.09.018

Aiuppa A, Federico C, Giudice G, Gurrieri S (2005b) Chemical mapping of a fumarolic field: La Fossa Crater, Vulcano Island (Aeolian Islands, Italy). Geophys Res Lett 32:L13309. doi:10.1029/2005GL023207

Aiuppa A, Federico C, Giudice G, Gurrieri S, Valenza M (2006) Hydrothermal buffering of the SO_2/H_2S ratio in volcanic gases: evidence from La Fossa Crater fumarolic field, Vulcano Island. Geophys Res Lett 33:L21315. doi:10.1029/2006GL027730

Aiuppa A, Bani P, Moussallam Y, Di Napoli R, Allard P, Gunawan H, Hendrasto M, Tamburello G (2015) First determination of magma-derived gas emissions from Bromo volcano, eastern Java (Indonesia). J Volcanol Geotherm Res 304:206–213. doi:10.1016/j.jvolgeores.2015.09.008

Allard P, Aiuppa A, Beauducel F, Gaudin D, Di Napoli R, Calbrese S, Parello F, Crispi O, Hammouya G, Tamburello G (2014) Steam and gas emission rate from La Soufriere volcano, Guadeloupe (Lesser Antilles): implications for the magmatic supply during degassing unrest. Chem Geol 384:76–93. doi:10.1016/j.chemgeo.2014.06.019

Amici S, Turci M, Giammanco S, Spampinao L, Giulietti F (2013) UAV thermal remote sensing of an Italian mud volcano. Adv Remote Sens 2:358–364

Bandy AR, Maroulis PJ, Wilner LA (1982) Estimates of the fluxes of NO, SO_2, H_2S, CS_2 and OCS from Mt. St. Helens deduced from in situ plume concentration measurements. Geophys Res Lett 99:1097–1100

Barberi F, Bertagnini A, Landi P, Principe C (1992) A review on phreatic eruptions and their precursors. J Volcanol Geotherm Res 52(4):231–246. doi:10.1016/0377-0273(92)90046-G

Burton MR, Oppenheimer C, Horrocks LA, Francis PW (2000) Remote sensing of CO_2 and H_2O emission rates from Masaya volcano, Nicaragua. Geology 28(10):915–918

Doukas MP, McGee KA (2007) A compilation of gas emission-rate data from volcanoes of cook Inlet (Spurr, Crater Peak, Redoubt, Iliamna, and Augustine) and Alaska Peninsula (Douglas, Fourpeaked, Griggs, Mageik, Martin, Peulik, Ukinrek Maars, and Veniaminof), Alaska, from 1995–2006. U.S. Geological Survey Open-File Report 2007–1400

Earthquake Research Institute of the University of Tokyo (2014) http://www.data.jma.go.jp/svd/vois/data/tokyo/STOCK/kaisetsu/CCPVE/shiryo/130/130_no01.pdf. Accessed 20 Oct 2015

Ellis AJ, Giggenbach W (1971) Hydrogen sulphide ionization and sulphur hydrolysis in high temperature solution. Geochim Cosmochim Acta 35:247–260

Galle B, Oppenheimer C, Geyer A, McGonigle AJS, Edmonds M, Horrocks LA (2003) A miniaturized ultraviolet spectrometer for remote sensing of SO_2 fluxes: a new tool for volcano surveillance. J Volcanol Geotherm Res 119:241–254

Galle B, Johansson M, Rivera C, Zhang Y, Kihlman M, Kern C, Lehmann T, Platt U, Arellano S, Hidalgo S (2010) Network for observation of volcanic and atmospheric change (NOVAC)—a global network for volcanic gas monitoring: network layout and instrument description. J Geophys Res 115:D05304. doi:10.1029/2009JD011823

Giggenbach WF (1987) Redox processes governing the chemistry of fumarolic gas discharges from White Island, New Zealand. Appl Geochem 2:143–161

Hobbs PV, Radke LF, Eltgroth MW, Hegg DA (1981) Airborne studies of the emissions from the volcanic eruptions of Mount St. Helens. Science 211:816–818

Hobbs PV, Tuell JP, Hegg DA, Radke LF, Eltgroth MW (1982) Particles and gases in the emissions from the 1980-81 eruptions of Mount St. Helens. J Geophys Res 87:11062–11086

Horton KA, Williams-Jones G, Garbeil H, Elias T, Sutton AJ, Mouginis-Mark P, Porter JN, Clegg S (2006) Real-time measurement of volcanic SO_2, emissions: validation of a new UV correlation spectrometer (FLYSPEC). Bull Volcanol 68:323–327

Iwasaki I, Ozawa T, Yoshida M, Iwasaki B, Kamada M (1966) Differentiation of magmatic emanation. Bull Tokyo Inst Tech 74:1–57

Jaeschke W, Berresheim H, Georgii H-W (1982) Sulfur emissions from Mt. Etna. J Geophys Res 87:7253–7261

JMA (2014a) In: Bulletins on volcanic activity (September 2014). http://www.data.jma.go.jp/svd/vois/data/tokyo/STOCK/monthly_v-act_doc/tokyo/14m09/312_14m09.pdf. Accessed on 12 Nov 2015

JMA (2014b) In: Bulletins on volcanic activity (October 2014). http://www.data.jma.go.jp/svd/vois/data/tokyo/STOCK/monthly_v-act_doc/tokyo/14m09/312_14m09.pdf. Accessed on 12 Nov 2015

JMA (2015) In: Bulletins on volcanic activity (October 2015). http://www.data.jma.go.jp/svd/vois/data/tokyo/STOCK/monthly_v-act_doc/tokyo/15m10/312_15m10.pdf. Accessed on 12 Nov 2015

Jordan BR (2015) A bird's eye view of geology: the use of micro drones/UAVs in geologic field work and education. GSA Today 25:50–52. doi:10.1130/GSATG232GW.1

Kaneko T, Koyama T, Yasuda A, Takeo M, Yanagisawa T, Kajiwara K, Honda Y (2011) Low-altitude remote sensing of volcanoes using an unmanned autonomous helicopter: an example of aeromagnetic observation at Izu-Oshima volcano, Japan. Int J Remote Sens 32:1491–1504

Kato A, Terakawa T, Yamanaka Y, Maeda Y, Horikawa S, Matsuhiro K, Okuda T (2015) Preparatory and precursory process leading up to the 2014 phreatic eruption of Mount Ontake, Japan. Earth Planets Space 67:111. doi:10.1186/s40623-015-0288-x

Kelly PJ, Kern C, Roberts TJ, Lopez T, Werner C, Aiuppa A (2013) Rapid chemical evolution of tropospheric volcanic emissions from Redoubt Volcano, Alaska, based on observations of ozone and halogen-containing gases. J Volcanol Geotherm Res 259:317–333

Kobayashi T (1979) 1979 Eruption of Ontake volcano, Central Japan. Earth Science (Chikyu kagaku) The Journal of the Association for the Geological Collaboration in Japan 33(6):ii–ib

Maeno F, Nakada S, Kaneko T (2014) Volumes of the 2014 and 1979 eruptions at Ontake volcano, central Japan. In: Programme and Abstracts The Volcanological Society of Japan 2014 Fall Meeting, Fukuoka University, Fukuoka, Japan, 2–4 Nov 2014

Mather TA, Pyle DM, Tsanev VI, McGonigle AJS, Oppenheimer C, Allen AG (2006) A reassessment of current volcanic emissions from the Central American arc with specific examples from Nicaragua. J Volcanol Geotherm Res 149:297–311

McGee KA, Doukas MP, Gerlach TM (2001) Quiescent hydrogen sulfide and carbon dioxide degassing from Mount Baker, Washington. Geophys Res Lett 28:4479–4482

McGonigle AJS, Aiuppa A, Giudice G, Tamburello G, Hodson AJ, Gurrieri S (2008) Unmanned aerial vehicle measurements of volcanic carbon dioxide fluxes. Geophys Res Lett 35:L06303. doi:10.1029/2007GL032508

NASA-GSFC and Michigan Tech Univ (2014) http://SO2.gsfc.nasa.gov/pix/special/2014/ontake/141001OntakeOMPS-E.html. Accessed on 3 Feb 2016

Mori T, Kato K (2013) Sulfur dioxide emissions during the 2011 eruption of Shinmoedake volcano, Japan. Earth Planets Space 65:573–580. doi:10.5047/eps.2013.04.005

Mori T, Notsu K (1997) Remote CO, COS, CO_2, SO_2, HCl detection and temperature estimation of volcanic gas. Geophys Res Lett 24(16):2047–2050. doi:10.1029/97GL52058

Mori T, Hirabayashi J, Kazahaya K, Mori T, Ohwada M, Miyashita M, Iino H, Nakahori Y (2007) A compact ultraviolet spectrometer system (COMPUSS) for monitoring volcanic SO_2 emission: validation and preliminary observation. Bull Volcanol Soc Japan 52:105–112

Nakamichi H, Kumagai H, Nakano M, Okubo M, Kimata F, Ito Y, Obara K (2009) Source mechanism of very-long-period event at Mt. Ontake, central Japan: response of a hydrothermal system to magma intrusion beneath the summit. J Volcanol Geotherm Res 187:167–177

Oana S, Ishikawa H (1966) Sulfur isotopic fraction between sulfur and sulfuric acid in the hydrothermal solution of sulfur dioxide. Geochem J 1:45–50

Oikawa T (2008) Reinvestigation of the historical eruption and fumarolic activity records at Ontake volcano, central Japan. Misunderstanding reports about the 774 AD and 1892 AD eruptions. Bull Geol Surv Japan 59:203–210

Oikawa T (2013) 53 Ontakesan. In: Japan Meteorological Agency, Volcanological Society of Japan (eds) National catalogue of the active volcanoes in Japan (4th edn, English Version) http://www.data.jma.go.jp/svd/vois/data/tokyo/STOCK/souran_eng/volcanoes/053_ontakesan.pdf. Accessed 23 Sept 2015

Oikawa T, Okuno M (2009) Recent volcanic history of Ontake Volcano, central Japan. In: Abstracts of Japan Geoscience Union Meeting 2009, Makuhari Messe, Chiba, Japan, 16–21 May 2009

Oppenheimer C (2003) Volcanic degassing. In: Rudnick RL (ed) The crust. and Holland HD, Turekian KK (eds) Treatise on geochemistry, vol 3. Elsevier, Amsterdam, pp 123–166

Oppenheimer C (2010) Ultraviolet sensing of volcanic sulfur emissions. Elements 6:87–92. doi:10.2113/gselements.6.2.87

Oppenheimer C, Scaillet B, Martin RS (2011) Sulfur degassing from volcanoes: source conditions, surveillance, plume Chemistry and earth system impacts. Rev Mineral Geochem 73:363–421. doi:10.2138/rmg.2011.73.13

Ossaka J, Ozawa T, Sakai H, Hirabayashi J (1983) Geochemical study on the volcanic activity of Kiso-Ontake volcano, after the 1979 eruption. Bull Volcanol Soc Japan 28:59–74

Radke LF, Hobbs PV, Stith JL (1976) Airborne measurements of gases and aerosols from volcanic vents on Mt. Baker. Geophys Res Lett 32:93–96

Sano Y, Nakamura Y, Wakita H, Urabe A, Tominaga T (1984) Helium-3 emission related to volcanic activity. Science 224:150–151
Sano Y, Nakamura Y, Wakita H, Notsu K, Kobayashi Y (1986) 3He/4He ratio anomalies associated with the 1984 western Nagano earthquake: possibly induced by a diapiric magma. J Geophys Res 91:12291–12295
Sano Y, Kagoshima T, Takahata N, Nishio Y, Roulleau E, Pinti DL, Fischer TP (2015) Ten-year helium anomaly prior to the 2014 Mt. Ontake eruption. Sci Rep 5:13069. doi:10.1038/srep13069
Shinohara H (2005) A new technique to estimate volcanic gas composition: plume measurements with a portable multi-sensor system. J Volcanol Geotherm Res 143:319–333
Shinohara H (2013) Composition of volcanic gases emitted during repeating Vulcanian eruption stage of Shinmoedake, Kirishima volcano, Japan. Earth Planets Space 65:667–675. doi:10.5047/eps.2012.11.001
Shinohara H, Matsushima N, Kazahaya K, Ohwada M (2011) Magma-hydrothermal system interaction inferred from volcanic gas measurements obtained during 2003–2008 at Meakandake volcano, Hokkaido, Japan. Bull Volcanol 73:409–421
Soya T, Kondo Y, Shimosaka K (1980) The 1979 eruption of Mt. Ontake. Chishitu News 306:6–13. https://www.gsj.jp/data/chishitsunews/80_02_01.pdf Accessed 24 Nov 2015
Stoiber RE, Malinconico LL, Williams SN (1983) Use of the correlation spectrometer at volcanoes. In: Tazieff H, Sabroux J-C (eds) Forecasting volcanic events. Elsevier, Amsterdam, pp 425–444
Sugiura T, Sugisaki R, Mizutani Y, Kusakabe M (1980) Geochemistry of volcanic ashes, thermal waters and gases ejected during the 1979 eruption of Ontake volcano, Japan. Bull Volcanol Soc Japan 25:231–244
Sugiura T, Morishita S, Kato K (1997) Chemical compositions of volcanic gases from Mt. Ontake. Bull Aichi Univ Educ Nat Sci 46:5–12
Suzuki Y, Tanaka M, Chiba T, Shioya M, Itou T (2007) Discovery and meaning of the scoriaflow deposit about 5000 years before on Northwestern slope of the Ontake volcano. In: Abstracts of Japan Geoscience Union Meeting 2007, Makuhari Messe, Chiba, Japan, 19–24 May 2007
Suzuki Y, Chiba T, Kishimoto H, Okamoto A (2009) Recent eruptive history of younger Ontake volcano, Japan. In: Abstracts of Japan geoscience union meeting 2009, Makuhari Messe, Chiba, Japan, 16–21 May 2009
Symonds RB, Gerlach TM, Reed MH (2001) Magmatic gas scrubbing: implications for volcano monitoring. J Volcanol Geotherm Res 108:303–341
Werner C, Hurst T, Scott B, Sherburn S, Chrestenson BW, Bretten K, Cole-Baker J, Mullan B (2008) Variability of passive gas emissions, seismicity, and deformation during crater lake growth at White Island Volcano, New Zealand, 2002–2006. J Geophys Res 113:B01204. doi:10.1029/2007JB005094
Werner C, Kelly PJ, Doukas M, Lopez T, Pfeffer M, McGimsey R, Neal C (2013) Degassing of CO_2, SO_2, and H_2S associated with the 2009 eruption of Redoubt Volcano, Alaska. J Volcanol Geotherm Res 259:270–284. doi:10.1016/j.jvolgeores.2012.04.012
Yamaoka K (2015) The 2014 Mt. Ontake eruption. J JSNDS 33:330–346